ISBN: 978-3-95450-247-9 ISSN: 2673-5490 doi: 10.18429/JACoW-IPAC2024-MOPR86

EMPIRICAL MODELING OF THE PHOTOCURRENT TIME-DEPENDENCE IN CO-DEPOSITION ACTIVATION PROCEDURES FOR GaAs PHOTOCATHODES*

M. Herbert†, J. Enders, M. Engart, M. Meier, J. Schulze, V. Wende
Institut für Kernphysik, Fachbereich Physik, Technische Universität Darmstadt, Darmstadt, Germany

Abstract

GaAs-based photocathodes can provide electron beams with high spin-polarization. In order to be used in a photogun for high-current applications such as energy-recovery linacs and colliders, the quantum efficiency as well as the lifetime of the photocathode need to be as high as possible. Both parameters depend on the quality of the thin layer that is applied to the photocathode surface during the so-called activation process in order to create negative electron-affinity conditions for optimal photoemission. Hence, it is of great interest to optimize and standardize this procedure in order to provide the best possible photocathode performance for accelerator applications.
For an automatization of the activation process it is necessary to model the photocurrent as a function of time during the process. To this end, activations of bulk-GaAs using Cs and O_2, conducted at the Photo-CATCH test stand, were analysed using an empirical model function. This contribution presents the results of the analysis and its implications regarding the influence of the activation process on the performance of the activated photocathode.

INTRODUCTION

The superconducting Darmstadt linear accelerator S-DALINAC [1] is operated at the Institut für Kernphysik (IKP) at TU Darmstadt [2]. Its thrice-recirculating lattice design is capable of single- and multi-turn energy recovery operation [3,4] and features two electron sources: a thermionic gun for unpolarized beam and a DC photo-electron gun with negative electron-affinity (NEA) GaAs-based photocathodes, situated at the S-DALINAC polarized injector SPIn, [5] for spin-polarized beam.
Future applications of spin-polarized electron beams at the S-DALINAC, such as polarization transfer and correlation studies [6], require photocathodes with optimized operational parameters, most importantly quantum efficiency η and lifetime τ. A separate test stand for photo-cathode activation, test and cleaning using atomic hydrogen Photo-CATCH is available [7], enabling studies on photocathode parameters [8–11] as well as research on photogun development [12] independent of beam time at the S-DALINAC. The test stand features a dedicated activation chamber, a gun chamber with a −60 kV inverted-insulator geometry DC photo-gun, and an adjacent beamline for beam parameter analysis.

* Work supported by DFG (GRK 2128 "AccelencE", project number 264883531)
† mherbert@ikp.tu-darmstadt.de

Previous studies at Photo-CATCH on the automatization of the activation process have shown that a precise control of the procedure is necessary to improve the reliability of the automated scheme [10]. For this purpose, an analysis of the photocurrent time dependence was conducted for the co-deposition (Co-De) procedure commonly used at Photo-CATCH. The resulting empirical model and preliminary implications derived from it are presented in this contribution.

ACTIVATION PROCEDURE

NEA activations of GaAs photocathodes at Photo-CATCH are carried out in the activation chamber using the Co-De method: after heat-cleaning the sample at temperatures between 610 °C and 650 °C for about 1 h, the sample is illuminated with a white light LED array and Cs is introduced via applying a current I_{cs} to a dispenser. An increase in photocurrent up to a saturation peak, the so-called Cs peak, is observed. Once the current has receded to about 75 % of the peak value, O_2 is introduced via applying a voltage U_{ox} to a piezo-electric leak valve. Again, an increase in photocurrent is observed up to a saturation peak, at which point both Cs and O_2 exposure is stopped. For measurement of η and τ, the LED array is switched off and the laser shutter is opened, introducing laser light with a wavelength of (785 ± 2) nm and power between 40 µW and 60 µW.
Two variants of the Co-De method are conducted at Photo-CATCH:

a) Upon O_2 introduction, U_{ox} is set such that the pressure within the chamber is rapidly increased to a pre-defined value and then kept approximately constant over time by carefully adjusting U_{ox}. This is done to keep the rate of O_2 exposure approximately constant. An example for the observed trend in photocurrent and pressure is shown in Fig. 1. This variant is referred to as *scheme 1a*.

b) During O_2 exposure, U_{ox} is kept at a constant setting. This leads to a pressure rise, corresponding to an increase in the amount of O_2 introduced into the chamber during activation. An example for the observed trend in photocurrent and pressure is shown in Fig. 2. This variant is referred to as *scheme 1b*.

While scheme 1a was previously optimized at Photo-CATCH [9], scheme 1b has only been introduced recently for further development of an automated

ISBN: 978-3-95450-247-9 ISSN: 2673-5490 doi: 10.18429/JACoW-IPAC2024-MOPR86

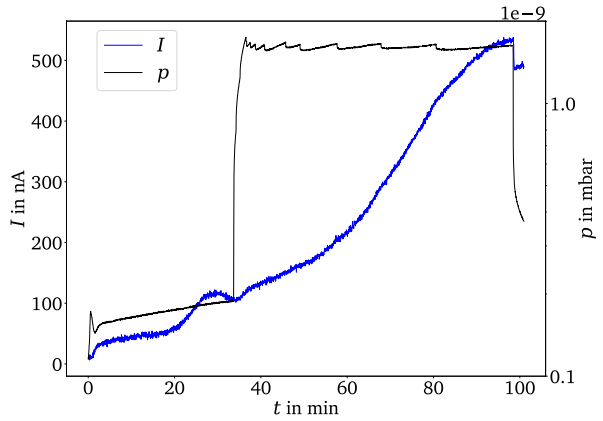

Figure 1: Anode current and pressure trend during a scheme 1a Co-De activation procedure at Photo-CATCH. The step in the current at about 100 min was caused by switching off the Cs dispencer and hence removing the background current. The activation yielded a final quantum efficiency of (9.74 ± 0.03) %.

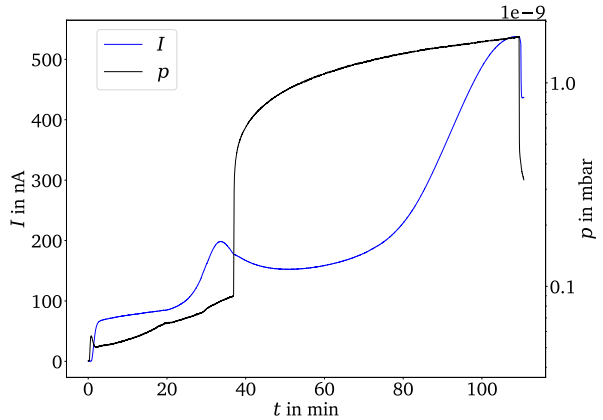

Figure 2: Anode current and pressure trend during a scheme 1b Co-De activation procedure at Photo-CATCH. The step in the current at about 110 min was caused by switching off the Cs dispencer and hence removing the background current. The activation yielded a final quantum efficiency of (5.30 ± 0.03) %.

activation scheme [10] and has not been optimized yet. Therefore, at 785 nm this scheme so far only achieved between 4 % and 7 %, compared to 7 % to 10 % previously achieved with scheme 1a [9]. The digital multimeter used previously to measure the anode current (see [9]) has recently been replaced by a new currentmeter, yielding a much smoother photocurrent curve, as can be seen when comparing the photocurrent trends in Fig. 1 and Fig. 2.

EMPIRICAL MODEL

First attempts to fit the photocurrent curve of a scheme 1a activation process with a continuous function were made in order to replicate activation data for test purposes. While such a function can be used to approximately reproduce the photocurrent trend during activation, it proved to be limited when attempting to fit activation data. Further analysis revealed that the photocurrent trend can be spearated into three distinct parts:

1) Background from Cs dispenser
Upon applying a current to the Cs dispenser, a short, steep rise in the current measured at the anode is observed, followed by a small but steady linear increase in current over time. Since this current occurs irrespective of cathode illumination, it is strictly speaking not part of the photocurrent trend, but instead background current, most likely caused by the emission of Cs ions from the dispenser or leak currents between dispenser and anode. Excluding the initial steep rise commonly observed within the first few minutes, this background current can be fitted with a linear approximation:

$$I_{\mathrm{bg}}(t) = m_{\mathrm{bg}} \cdot t + I_{\mathrm{off,bg}} \quad . \tag{1}$$

2) Cs peak
The first photocurrent saturation peak caused by adsoption of Cs on the photocathode surface can be described using a Gaussian function:

$$I_p(t) = a_{\mathrm{cs}} \cdot e^{-\frac{(t-\mu_{\mathrm{cs}})^2}{2\sigma_{\mathrm{cs}}^2}} \quad , \tag{2}$$

with the peak amplitude a_{cs}, temporal position μ_{cs} and width σ_{cs}. Taking into account the offset caused by the background current yields the function

$$I_p(t) = a_{\mathrm{cs}} \cdot e^{-\frac{(t-\mu_{\mathrm{cs}})^2}{2\sigma_{\mathrm{cs}}^2}} + m_{\mathrm{bg}} \cdot t + I_{\mathrm{off,bg}} \quad . \tag{3}$$

3) Co-De peak
The photocurrent trend during Co-De of Cs and O_2 can be fitted using a Gaussian function:

$$I_p(t) = a_{\text{co-de}} \cdot e^{-\frac{(t-\mu_{\text{co-de}})^2}{2\sigma_{\text{co-de}}^2}} + I_{\text{off,co-de}} \quad , \tag{4}$$

with the peak amplitude $a_{\text{co-de}}$, temporal position $\mu_{\text{co-de}}$ width $\sigma_{\text{co-de}}$ and offset $I_{\text{off,co-de}}$. While adjusting O_2 to the intended level directly after introduction, a deviation from the Gaussian shape of the Co-De peak can be observed. This can be described by adding a second Gaussian function:

$$\begin{aligned} I_p(t) = {} & a_{\text{co-de,1}} \cdot e^{-\frac{(t-\mu_{\text{co-de,1}})^2}{2\sigma_{\text{co-de,1}}^2}} \\ & + a_{\text{co-de,2}} \cdot e^{-\frac{(t-\mu_{\text{co-de,2}})^2}{2\sigma_{\text{co-de}}^2}} + I_{\text{off,co-de,2}} \quad . \end{aligned} \tag{5}$$

The resulting combined function allows a smooth fit of the Co-De peak. Here, the first Gaussian function describes the deviation after O_2 introduction and the second Gaussian function describes the general shape of the Co-De peak.

ISBN: 978-3-95450-247-9 ISSN: 2673-5490 doi: 10.18429/JACoW-IPAC2024-MOPR86

Upon introducing O_2, the photocurrent trend instantly changes course. This point proved to be problematic when trying to apply a uniform fit function to the entire activation curve. Hence, the activation curve needs to be separated into two sections that are then fitted separately:

i) Cs deposition, consisting of parts 1) and 2)

ii) Co-De of Cs and O_2, i.e. part 3)

Using this model, an accurate fit of scheme 1a activation curves was obtained, as shown exemplary in Fig. 3. Fitting the model to scheme 1b activation data also yielded good results, as shown exemplary in Fig. 4.

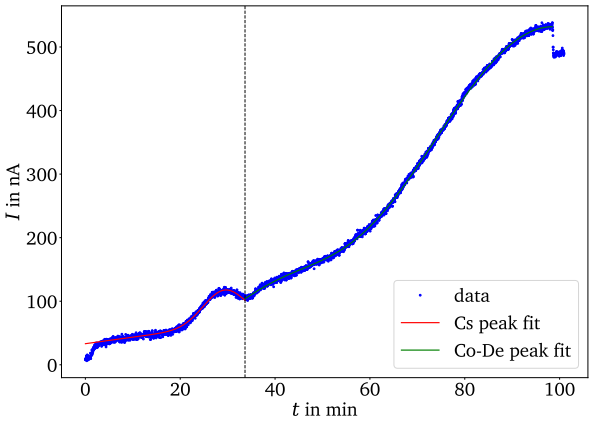

Figure 3: Anode current trend and fitted functions for sections i) (red) and ii) (green) of a scheme 1a activation process. The dashed vertical line marks the border between section i) (left) and section ii) (right) of the activation process.

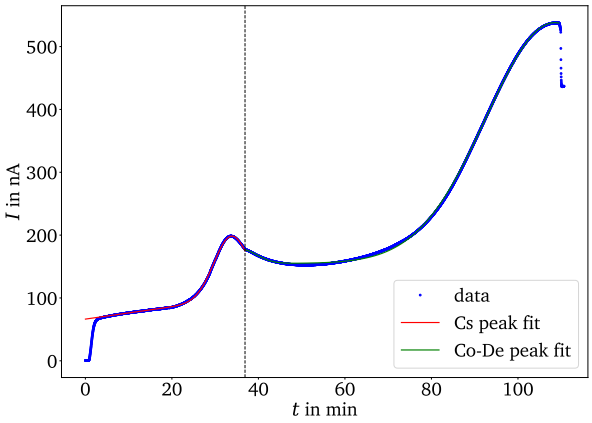

Figure 4: Anode current trend and fitted functions for sections i) (red) and ii) (green) of a scheme 1b activation process. The dashed vertical line marks the border between section i) (left) and section ii) (right) of the activation process.

PRELIMINARY ANALYSIS OF ACTIVATION DATA

Fitting the empirical model to the scheme 1a activation data presented in [9] yielded overall good agreements with the photocurrent trend. For section i), an increase in both m_{bg} and $I_{off,bg}$ over the course of several activations was observed. The slope increased from approximately 0 to about 1.7 nA min^{-1}, while the offset current increased from approximately 24 nA to about 71 nA. In reverse, a_{cs} decreased from approximately 50 nA to about 20 nA, comparable to the drop of Cs partial pressure that has been observed in [9]. The temporal position μ_{cs} increased over time, from about 20 min to nearly 35 min. This delay of the Cs saturation peak coincides with the decrease of Cs partial pressure. Hence, the assumption that the introduced amount of Cs greatly influences the timing of the activation process was confirmed. It was observed that the shape of the photocurrent trend in section ii) was not uniform due to different manual adjustment of the O_2 exposure during each activation process, limiting the comparability of the resulting fit parameters and hence impeding further analysis. The low quality of the anode current signal also had a negative impact.

Preliminary evaluation of scheme 1b activations showed good agreement of the model for both sections of the activation process so far. For section i), the model yielded a background function with m_{bg} ranging from 0.7 nA min^{-1} to 1.1 nA min^{-1} and $I_{off,bg}$ in the range of 45 nA to 66 nA. The parameters for the Cs saturation peak showed little variation, with $a_{cs} = (98 \pm 1)$ nA, μ_{cs} between 30 min and 34 min and $\sigma_{cs} = (4.1 \pm 0.1)$ min.

The fit to section ii) yielded high variations for the first Gaussian peak describing the initial decline in photocurrent directly after the start of O_2 exposure, with $a_{co\text{-}de,1}$ ranging from 2 nA to 23 nA, $\mu_{co\text{-}de,1}$ between 36 min and 48 min and $\sigma_{co\text{-}de,1}$ between 2.3 min and 3.7 min. The second Gaussian function describing the rise in photocurrent from Co-De of Cs and O_2 yielded an increase in $\mu_{co\text{-}de,2}$ from about 90 min to 110 min over the course of several activations, with a steady $\sigma_{co\text{-}de,2} = (15.5 \pm 0.5)$ min. The spread of $a_{co\text{-}de,2}$ between 380 nA and 470 nA appears to correlate to the observed variation in quantum efficiency, with a corresponding spread between 5.3 % and 6.9 %.

CONCLUSION AND OUTLOOK

An empirical model for the photocurrent trend during the Co-De activation process for GaAs photocathodes, consiting of two parts, has been found. Preliminary evaluation of two different variations of the activation procedure shows good agreement of the model with the data. Further analysis is required to determine if the resulting fit parameters can be used to predict the final photocathode performance.

REFERENCES

[1] A. Richter, "Operational experience at the S-DALINAC", in *Proc. EPAC'96*, Barcelona, Spain, Jun. 1996, pp. 110–114. https://tubiblio.ulb.tu-darmstadt.de/2551/

[2] N. Pietralla, "The Institute of Nuclear Physics at the TU Darmstadt", in *Nucl. Phys. News*, vol. 28, no. 2, pp. 4–11, 2018. doi:10.1080/10619127.2018.1463013

ISBN: 978-3-95450-247-9 ISSN: 2673-5490 doi: 10.18429/JACoW-IPAC2024-MOPR86

[3] M. Arnold *et al.*, "First operation of the superconducting Darmstadt linear electron accelerator as an energy recovery linac", in *Phys. Rev. Accel. Beams*, vol. 23, no. 2, p. 020101, 2020. doi:10.1103/PhysRevAccelBeams.23.020101

[4] F. Schließmann *et al.*, "Realization of a multi-turn energy recovery accelerator", in *Nat. Phys.*, vol. 19, pp. 597–602, 2023. doi:10.1038/s41567-022-01856-w

[5] Y. Poltoratska *et al.*, "Status and recent developments at the polarized-electron injector of the superconducting Darmstadt electron linear accelerator S-DALINAC", in *J. Phys.: Conf. Proc.*, vol. 298, p. 012002, 2011. doi:10.1088/1742-6596/298/1/012002

[6] J. Enders, "Ideas for fundamental electron scattering at the S-DALINAC", *AIP Conf. Proc.*, vol. 1563, pp. 223–226, 2013. doi:10.1063/1.4829415

[7] N. Kurichiyanil, "Design and construction of a test stand for photocathode research and experiments", Ph.D. thesis, Phys. Dept., Technische Universität Darmstadt, Darmstadt, Germany, 2017. https://tuprints.ulb.tu-darmstadt.de/5903/

[8] N. Kurichiyanil, J. Enders, Y. Fritzsche, and M. Wagner, "A test system for optimizing quantum efficiency and dark lifetime of GaAs photocathode", in *J. Instr.*, vol. 14, p. P08025, 2019. doi:10.1088/1748-0221/14/08/p08025

[9] M. Herbert, "Electron emission from GaAs photocathodes using conventional and Li-enhanced activation procedures", Ph.D. thesis, Phys. Dept., Technische Universität Darmstadt, Darmstadt, Germany, 2022. doi:10.26083/tuprints-00020707

[10] M. Herbert, T. Eggert, J. Enders, M. Engart, Y. Fritzsche, and V. Wende "Automated Activation Procedure for GaAs Photocathodes at Photo-CATCH" in *Proc. Sci.*, vol. 433, p. 3, 2023. doi:10.22323/1.433.0003

[11] M. Herbert, T. Eggert, J. Enders, M. Engart, Y. Fritzsche, M. Meier, J. Schulze, and V. Wende "Negative Electron-Affinity Activation Procedures for GaAs Photocathodes at Photo-CATCH" in *Proc. IPAC'23*, Venice, Italy, May 2023, pp. 1415–1417. doi:10.18429/JACoW-IPAC2023-TUPA035

[12] M. Herbert, J. Enders, Y. Fritzsche, N. Kurichiyanil, and V. Wende, "Inverted Geometry Photo-Electron Gun Research and Development at TU Darmstadt", in *Proc. IPAC'18*, Vancouver, BC, Canada, Apr.-May 2018, pp. 4545–4547. doi:10.18429/JACoW-IPAC2018-THPMK101